Hindawi
Journal of Robotics
Volume 2018, Article ID 8641731, 12 pages
https://doi.org/10.1155/2018/8641731

*Research Article*

# Mathematical Modeling and Modal Switching Control of a Novel Tiltrotor UAV

**Zhiwei Kong and Qiang Lu**

*School of Automation, Hangzhou Dianzi University, Hangzhou, China*

Correspondence should be addressed to Qiang Lu; lvqiang@hdu.edu.cn

Received 17 May 2018; Accepted 26 July 2018; Published 7 August 2018

Academic Editor: L. Fortuna



This paper concentrates on the flight control of a novel tiltrotor aircraft with fixed wings. This kind of aircraft has two flight modes and a transition mode. In the phase of vertical take off and landing (VTOL), the aircraft can operate as a quadrotor helicopter. And in the phase of horizontal flight, the aircraft is in the normal airplane mode. The transition mode is between these two flight modes. In this part of work, a novel tiltrotor aircraft was presented since transition mode is achieved by tilting the front dual tiltrotor (DTR) and the mathematical model was established. The classical PID method was used during the phase of VTOL and the numerical results were given and the simulation shows good control effect. A nonlinear control law based on backstepping was proposed to achieve a stable transition from vertical flight to horizontal flight. And the numerical results show that the flight mode could transit stably which shows the effectiveness of the control approach. Finally, the vertical flight experiment has been carried out on DTR aircraft and the attitude was stable.

## 1. Introduction

Tiltrotor aircraft attracted much researchers' attention in the field of aeronautics and astronautics since 1980s [1, 2]. The reason that tiltrotors have received such great attention is mainly because they combine the advantages of helicopters and fixed-wing aircraft [3, 4]. Helicopters can take off and land vertically, but they cannot fly horizontally at a high speed. Fixed-wing aircrafts can fly horizontally at a high speed, but they need a runway for takeoff and landing [4, 5]. Tiltrotor aircraft has the advantages of both helicopter and fixed-wing aircraft, which makes it have a wide application scene.

Bell Helicopter company developed the V22 Osprey tiltrotor aircraft in the 1990s, which became the world's first tiltrotor aircraft. Osprey immediately received widespread attention because of its excellent performance. At present, tiltrotor aircrafts have achieved great success in military and civil fields [6]. In military aspects, tiltrotor aircrafts can be used as carrier-based aircrafts and can complete the transportation task in harsh environment, such as deserts and islands. In civil aspects, they are often used in the tasks of pesticide spraying, power patrol inspection, terrain exploration, and disaster relief.

In previous studies on multimodal aircraft, many researchers have focused on quad tilt-wing (QTW) unmanned aerial vehicle (UAV) [3, 7–11]. This kind of aircraft transfers from quadrotor helicopter to airplane by turning wings. Oner [2] developed the QTW vehicle and the dynamic model is derived by using Newton-Euler formulation. And a linear quadratic regulator (LQR) controller was proposed to stabilize vertical flight. Benkhoud [3] utilized Model Predictive Control (MPC) approach to stabilize vehicle attitude and track its trajectory. And the simulation results showed the effectiveness of the approach. In engineering practice, the most widely used regulator control law is proportional, integral, and derivative control, referred to as PID control. Hancer [8] estimated the disturbance with a disturbance observer and utilized PID controller for robust hovering control. And the effectiveness of the controller was verified through experiments and simulations. Another kind of aircraft with similar performance called quad tiltrotor (QTR) UAV also attracted widespread attention [5, 6, 12–15]. This kind of aircrafts switches flight modal by turning rotors.

In [12], a convertible QTR was designed and a nonlinear controller based on dynamic inversion was given. Moreover, the trajectory of the aircraft was tracked. Flores [4, 16] have done some work on this subject. In [4], a QTR model with fixed wings was presented and a nonlineared controller was also given which is based on saturations and Lyapunov. And from the numerical simulations the control strategy obtained satisfactory results.

Some studies on the vertical takeoff and landing of quadrotor helicopter have achieved good results [1, 17–21]. Sliding model controller was used in quadrotor helicopter altitude and attitude control [1, 22]. Xu [22] divided quadrotor helicopter model into actuated subsystem and underactuated subsystem. Furthermore, sliding mode control laws were designed for the two subsystems and the vehicle's altitude and attitude were stabilized. In [18], a feedback linearizing controller and backstepping-like control law was proposed to control vehicle's motion which is restricted to yaw and vertical motions.

In recent years, there have been a large number of studies on QTW and QTR. Most of them studied the horizontal and vertical flight of this type of aircraft. However, there are few studies on the transition process. Therefore, solving the problem of switching the flight modal stably for QTR or QTW has great practical significance.

In this paper, a novel tiltrotor aircraft model with dual tiltable rotors was proposed as you can see in Figures 1, 3, and 4. It can take off vertically with four rotors and after transition the vehicle can fly horizontally with the front dual rotors. And the back two rotors will stop when the transition mode is completed. The modal switching control strategy is showed in Figure 2. When the DTR is in the phase of VTOL, DTR's kinetics model is the same as the quadrotor helicopter and the attitude controller is the quadrotor helicopter attitude controller. After the DTR reaches the reference value, the decision-making module will switch the kinetics model and controller into transition modal at the same time. The remainder of this paper is arranged as follows. In Section 2, the DTR kinetics model will be presented. In Section 3, PID method was used to control the position and attitude of the vertical flight phase. In Section 4, a nonlinear controller will be designed to implement the transition. In Section 5, the takeoff experiment was carried out on DTR aircraft. In Section 6, we will give a conclusion about this part of work and point out deficiencies and future improvements.

## 2. The Mathematical Model of the Tiltrotor UAV

*2.1. Coordinate System and Force Analysis.* In order to establish the mathematical model of the aircraft and analyze the force, the inertial coordinate and body coordinate are introduced. As you can see in Figure 4, $C_w(x_w, y_w, z_w)$ is the inertial coordinate that the origin of the coordinate is any point in space and $x_w$ axis points north, $y_w$ axis points east, and the $z_w$ axis points vertically downwards to the center of the earth. $C_b(x_b, y_b, z_b)$ is the body coordinate that the origin of the coordinate is the center of the aircraft mass. $x_b$ points to the aircraft head, the $z_b$ axis is perpendicular to the $x_b$ axis and points to the earth, and the $y_b$ axis is determined by the right hand rule. The body coordinate is fixed relative to the fuselage and rotates as the aircraft rotates. The attitude angles $\psi, \theta, \phi$ represent yaw, pitch, and roll, respectively. The transformation matrix $\Gamma_{bw}$ from body coordinate to inertial coordinate is represented as

$$\Gamma_{bw} = \begin{bmatrix} c_\psi c_\theta & s_\phi s_\theta c_\psi - c_\phi s_\psi & c_\phi s_\theta c_\psi + s_\phi s_\psi \\ c_\theta s_\psi & s_\phi s_\theta s_\psi + c_\phi c_\psi & c_\phi s_\theta s_\psi - s_\phi c_\psi \\ -s_\theta & s_\phi c_\theta & c_\phi c_\theta \end{bmatrix} \tag{1}$$

where $c_\theta$ and $s_\theta$ represent $\cos\theta$ and $\sin\theta$, respectively.

The aircraft is mainly subjected to the pull of four rotors $T_i (i = 1, 2, 3, 4)$, gravity $mg$, wings lift $T_L$, and air drag $T_D$. The rotor tilting angle is expressed by $\alpha$, and then the pull along the $x_b$ axis can be expressed as

$$T_{px} = (T_1 + T_2)\sin(\alpha) \tag{2}$$

where $T_i = k\omega_i^2$ and $\omega_i$ is the rotors' angular velocity. And the pull along the $z_b$ axis can be expressed as

$$T_{pz} = (T_1 + T_2)\cos(\alpha) + T_3 + T_4 \tag{3}$$

The speed along the $x_b$ axis will keep increasing when the rotors are tilting. At this time, the lift of the wings and the air drag to the fuselage cannot be ignored. And the wings lift $T_L$ and the air drag $T_D$ can be calculated as follows [23]:

$$T_L = \frac{1}{2}\varepsilon\rho A V_{xz}^2 \tag{4}$$

$$T_D = p_1 V_{xz}^2 + p_2 V_{xz} \tag{5}$$

where $\varepsilon$ is the lift coefficient, $\rho$ is air density, A represents the area of the wing, and $p_1$ and $p_2$ are drag coefficient. $V_{xz}^2$ represents the vector sum of $x_b$ axis and $z_b$ axis velocity, i.e.,

$$V_{xz} = \sqrt{v_{bx}^2 + v_{bz}^2} \tag{6}$$

Suppose $L(\pm L_x, \pm L_y, \pm L_z)$ represents the coordinates of the rotor in the body frame; then the resultant force moment of the rotors $M_t = [M_x, M_y, M_z]^T$ can be expressed as

$$\begin{aligned} M_t &= \begin{bmatrix} T_1\sin\alpha \\ 0 \\ -T_1\cos\alpha \end{bmatrix} \times \begin{bmatrix} L_x \\ -L_y \\ -L_z \end{bmatrix} + \begin{bmatrix} T_2\sin\alpha \\ 0 \\ -T_2\cos\alpha \end{bmatrix} \times \begin{bmatrix} L_x \\ L_y \\ -L_z \end{bmatrix} \\ &\quad + \begin{bmatrix} 0 \\ 0 \\ -T_3 \end{bmatrix} \times \begin{bmatrix} -L_x \\ -L_y \\ -L_z \end{bmatrix} + \begin{bmatrix} 0 \\ 0 \\ -T_4 \end{bmatrix} \times \begin{bmatrix} -L_x \\ L_y \\ -L_z \end{bmatrix} \\ &= \begin{bmatrix} (-T_1\cos\alpha + T_2\cos\alpha - T_3 + T_4) L_y \\ -(T_1 + T_2)(L_x\cos\alpha - L_z\sin\alpha) + (T_3 + T_4) L_x \\ (-T_1 + T_2) L_y\sin\alpha \end{bmatrix} \end{aligned} \tag{7}$$

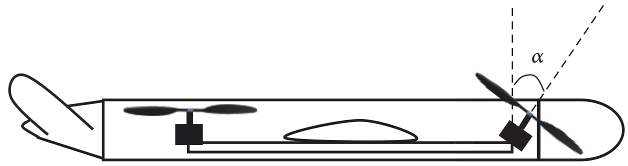


FIGURE 1: Tilting angle.

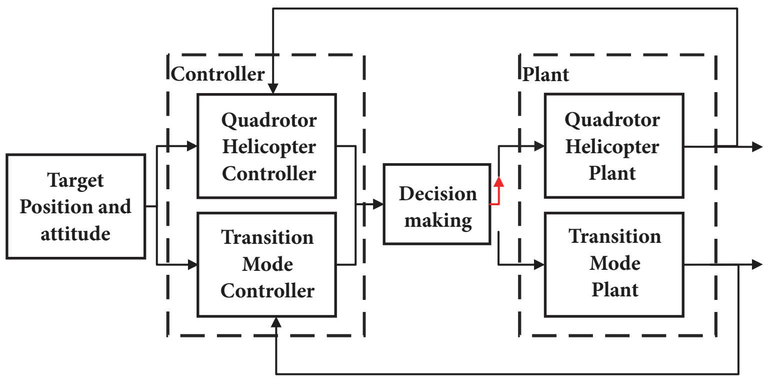


FIGURE 2: Modal switching control strategy.

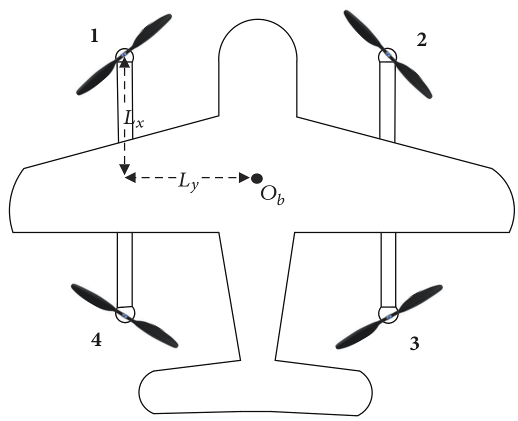


FIGURE 3: The top view of DTR.

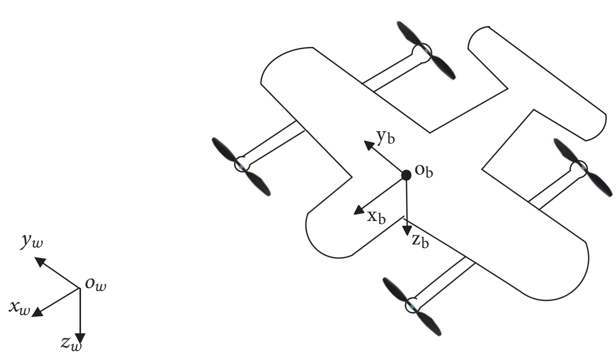


FIGURE 4: The inertial coordinate and body coordinate.

Assuming that air drag and lift act on the geometric center of the two wings, then the moment of air drag and lift can be expressed as

$$M_{ld} = \begin{bmatrix} -T_D \\ 0 \\ -T_L \end{bmatrix} \times \begin{bmatrix} 0 \\ -L_y \\ 0 \end{bmatrix} + \begin{bmatrix} -T_D \\ 0 \\ -T_L \end{bmatrix} \times \begin{bmatrix} 0 \\ L_y \\ 0 \end{bmatrix} = 0 \quad (8)$$

Due to the rotation of the rotors, the gyro effect and counteractive moment are produced. But when the tilting rotors have the same angular velocity as well as the fixed rotors, the gyro effect and counteractive moment will be eliminated. And in the following control strategy, the input $T_1 = T_2$ and $T_3 = T_4$ will be given. Therefore, the gyros effect and counteractive moment are not considered here. And gravity does not produce a moment due to it acts on the center of mass.

*2.2. Kinetics Model.* If $\nu(p, q, r)$ represents the aircraft roll, pitch, and yaw rates in body coordinates, $\gamma(I_x, I_y, I_z)$ represents the rotary inertia of body coordinates axis. From the Newton-Euler equation, the relationship of angular acceleration and moment can be expressed as

$$\begin{aligned} I_x\dot{p} + \left(I_z - I_y\right) qr &= \Sigma M_x \\ I_y\dot{q} + \left(I_x - I_z\right) rp &= \Sigma M_y \\ I_z\dot{r} + \left(I_y - I_x\right) pq &= \Sigma M_z \end{aligned} \quad (9)$$

substituting (7) into (9),

$$\begin{aligned} \dot{p} &= \frac{I_y - I_z}{I_x} qr - \frac{L_y \cos\alpha}{I_x}\left(-T_1 + T_2\right) \\ &\quad + \frac{L_y}{I_x}\left(-T_3 + T_4\right) \\ \dot{q} &= \frac{I_z - I_x}{I_y} rp - \frac{L_x \cos\alpha - L_z \sin\alpha}{I_y}\left(T_1 + T_2\right) \\ &\quad + \frac{L_x}{I_y}\left(T_3 + T_4\right) \\ \dot{r} &= \frac{I_x - I_y}{I_z} pq + \frac{L_y \sin\alpha}{I_z}\left(-T_1 + T_2\right) \end{aligned} \quad (10)$$

When the Euler angle is relatively small, it can be considered approximately as $p = \dot{\phi}$, $q = \dot{\theta}$, and $r = \dot{\psi}$.

According to Newton's second law $\overrightarrow{F} = m\overrightarrow{\dot{v}}$ and transforming the resultant force from body coordinate to inertial coordinate, the dynamic model of the aircraft can be expressed as

$$\begin{aligned} m\ddot{x} &= c_\psi c_\theta T_{px} - \left(s_\phi s_\psi + c_\psi s_\theta c_\phi\right)\left(T_{pz} + 2T_L\right) - c_\psi c_\theta T_D \\ m\ddot{y} &= c_\theta s_\psi T_{px} - \left(c_\phi s_\theta s_\psi - s_\phi c_\psi\right)\left(T_{pz} + 2T_L\right) \\ &\quad - c_\theta s_\psi T_D \\ m\ddot{z} &= -s_\theta T_{px} - c_\phi c_\theta\left(T_{pz} + 2T_L\right) + mg + s_\theta T_D \\ \ddot{\phi} &= c_1\dot{\theta}\dot{\psi} - c_2\cos\alpha\left(-T_1 + T_2\right) + c_3\left(-T_3 + T_4\right) \\ \ddot{\theta} &= c_4\dot{\psi}\dot{\phi} - \left(c_5\cos\alpha - c_6\sin\alpha\right)\left(T_1 + T_2\right) \\ &\quad + c_7\left(T_3 + T_4\right) \\ \ddot{\psi} &= c_8\dot{\phi}\dot{\theta} + c_9\sin\alpha\left(-T_1 + T_2\right) \end{aligned} \quad (11)$$

where $c_1 = (I_y - I_z)/I_x$, $c_2 = c_3 = L_y/I_x$, $c_4 = (I_z - I_x)/I_y$, $c_5 = c_7 = L_x/I_y$, $c_6 = L_z/I_y$, $c_8 = (I_x - I_y)/I_z$, $c_9 = L_y/I_z$.

## 3. Vertical Takeoff Control Approach

In the phase of vertical takeoff, the classic quadrotor PID control method was used. The tilting angle $\alpha = 0$ when the DTR takes off at a low speed. Therefore, air drag $T_D$ and wings lift $T_L$ will be ignored. The aircraft makes a small angle movement in the hovering state, and then the dynamic model can be expressed as

$$\begin{aligned} m\ddot{x} &= -\left(s_\phi s_\psi + c_\psi s_\theta c_\phi\right)\left(T_1 + T_2 + T_3 + T_4\right) \\ m\ddot{y} &= -\left(c_\phi s_\theta s_\psi - s_\phi c_\psi\right)\left(T_1 + T_2 + T_3 + T_4\right) \\ m\ddot{z} &= -c_\phi c_\theta\left(T_1 + T_2 + T_3 + T_4\right) + mg \\ \ddot{\phi} &= c_1\dot{\theta}\dot{\psi} + c_2\left(T_1 - T_2 - T_3 + T_4\right) \\ \ddot{\theta} &= c_4\dot{\psi}\dot{\phi} + c_5\left(-T_1 - T_2 + T_3 + T_4\right) \\ \ddot{\psi} &= c_8\dot{\phi}\dot{\theta} + c_9\left(-T_1 + T_2 - T_3 + T_4\right) \end{aligned} \quad (12)$$

The PID controller is a common feedback loop component in industrial control applications and consists of a proportional element P, an integral element I, and a derivative element D. The basis of PID control is proportional control, integral control can eliminate steady-state error but may increase overshoot, and derivative control can speed up large inertial system response speed and weaken overshoot trend.

The resultant force of the four rotors is used as the control input, and the dynamic model can be writen as

$$\begin{aligned} \ddot{x} &= \left(s_\phi s_\psi + c_\psi s_\theta c_\phi\right) u_1 \\ \ddot{y} &= \left(c_\phi s_\theta s_\psi - s_\phi c_\psi\right) u_1 \\ \ddot{z} &= c_\phi c_\theta u_1 + g \\ \ddot{\phi} &= c_1\dot{\theta}\dot{\psi} + u_2 \\ \ddot{\theta} &= c_4\dot{\psi}\dot{\phi} + u_3 \\ \ddot{\psi} &= c_8\dot{\phi}\dot{\theta} + u_4 \end{aligned} \quad (13)$$

The trajectory of the aircraft $(x, y, z)$ and the yaw $\phi$ were tracked only since this is an underactuated system. Furthermore, to track the desire attitude $\theta_d, \phi_d$, replace the virtual inputs $u_1$ in (13) as follows:

$$\begin{aligned} u_{x1} &= \left(s_\phi s_\psi + c_\psi s_\theta c_\phi\right) u_1 \\ u_{y1} &= \left(c_\phi s_\theta s_\psi - s_\phi c_\psi\right) u_1 \\ u_{z1} &= c_\phi c_\theta u_1 \end{aligned} \tag{14}$$

And the control law is designed as

$$\begin{aligned} u_{x1} &= -r_{xp}x - r_{xi}\int x dt - r_{xd}\dot{x} \\ u_{y1} &= -r_{yp}y - r_{yi}\int y dt - r_{yd}\dot{y} \\ u_{z1} &= -r_{zp}z_e - r_{zi}\int z_e dt - r_{zd}\dot{z}_e - g + \ddot{z}_d \end{aligned} \tag{15}$$

where $z_e = z - z_d$ and $z_d$ is the desire altitude. To satisfy the control law (15) the desired attitude angle $\theta_d, \phi_d$ should be tracked. The attitude angle error is defined as

$$\begin{aligned} \theta_e &= \theta - \theta_d, \\ \dot{\theta}_e &= \dot{\theta} - \dot{\theta}_d \\ \phi_e &= \phi - \phi_d, \\ \dot{\phi}_e &= \dot{\phi} - \dot{\phi}_d \end{aligned} \tag{16}$$

where $\theta_d, \phi_d$ can be calculated as

$$\begin{aligned} \theta_d &= \arcsin\left(\frac{c_\psi^2 u_{x1} + c_\psi s_\psi u_{y1}}{u_{z1}}\right) \\ \phi_d &= \arctan\left(\frac{c_\psi s_\psi u_{x1} - c_\psi^2 u_{y1}}{u_{z1}}\right) \end{aligned} \tag{17}$$

The attitude system control law is designed as

$$\begin{aligned} u_2 &= -r_{p2}\phi_e - r_{i2}\int \phi_e dt - r_{d2}\dot{\phi}_e + \ddot{\phi}_d \\ u_3 &= -r_{p3}\theta_e - r_{i3}\int \theta_e dt - r_{d3}\dot{\theta}_e + \ddot{\theta}_d \\ u_4 &= -r_{p4}\psi_e - r_{i4}\int \psi_e dt - r_{d4}\dot{\psi}_e + \ddot{\psi}_d \end{aligned} \tag{18}$$

The numerical results are showed in Figures 5, 6, 7, and 8. Figure 5 shows the aircraft's takeoff trajectory from (3,3) to (0,0) and the target altitude $z_d = 15$. Figure 6 shows the control inputs changes over time. In Figure 7, $\theta$ and $\phi$ converge to 0 and $\psi$ reaches the target value $\pi/6$. Figure 8 shows the position changes along the axis of the inertia coordinate. From the simulation results the PID control approach shows good control effect on attitude and position in vertical flight phase.

## 4. Transition Flight Control Approach

In the transition mode, rotor1 and rotor2 are always given the same input $T_1 = T_2$ as well as rotor3 and rotor4 $T_3 = T_4$. This input allocation method has a greater influence on $\theta$ than $\phi$ and $\psi$. Moreover, define the input $\tau_1 = T_1 = T_2$ and $\tau_2 = T_3 = T_4$. Therefore, the dynamic model during transition can be expressed as

$$\begin{aligned} \ddot{x} &= 2\tau_1 s_\alpha \frac{c_\psi c_\theta}{m} - \frac{2\left(s_\phi s_\psi + c_\psi s_\theta c_\phi\right)}{m}\left(\tau_1 c_\alpha + \tau_2 + T_L\right) \\ &\quad - \frac{c_\psi c_\theta}{m} T_D \\ \ddot{y} &= 2\tau_1 s_\alpha \frac{c_\theta s_\psi}{m} - \frac{2\left(c_\phi s_\theta s_\psi - s_\phi c_\psi\right)}{m}\left(\tau_1 c_\alpha + \tau_2 + T_L\right) \\ &\quad - \frac{c_\theta s_\psi}{m} T_D \\ \ddot{z} &= -2\tau_1 s_\alpha \frac{s_\theta}{m} - \frac{2c_\phi c_\theta}{m}\left(\tau_1 c_\alpha + \tau_2 + T_L\right) + g + \frac{s_\theta}{m} T_D \\ \ddot{\phi} &= c_1\dot{\theta}\dot{\psi} \\ \ddot{\theta} &= c_4\dot{\psi}\dot{\phi} - 2\tau_1\left(c_5 c_\alpha - c_6 s_\alpha\right) + 2c_7\tau_2 \\ \ddot{\psi} &= c_8\dot{\phi}\dot{\theta} \end{aligned} \tag{19}$$

When the rotors tilting angle change from 0 to $\pi/2$, the key point to design the control law is to keep the height of the aircraft from falling and the pitch angle $\theta$ should be close to 0. That means the resultant force on the $z_w$ axis should be in the negative direction, i.e.,

$$s_\theta T_{px} + c_\phi c_\theta\left(T_{pz} + 2T_L\right) + s_\theta T_D \geqq mg \tag{20}$$

Therefore, to realize the tilting process stably the main task under this input strategy is to control the following subsystem:

$$\begin{aligned} \ddot{z} &= -2\tau_1 s_\alpha \frac{s_\theta}{m} - \frac{2c_\phi c_\theta}{m}\left(\tau_1 c_\alpha + \tau_2 + T_L\right) + g + \frac{s_\theta}{m} T_D \\ \ddot{\theta} &= c_4\dot{\psi}\dot{\phi} - 2\tau_1\left(c_5 c_\alpha - c_6 s_\alpha\right) + 2c_7\tau_2 \end{aligned} \tag{21}$$

In addition, at the equilibrium point of the system $\sin\theta \approx \theta$, $\cos\theta \approx 1$. Then, the nonlinear system is partially linearized as follows:

$$\begin{aligned} \ddot{z} &= -2\tau_1 s_\alpha \frac{\theta}{m} - \frac{2c_\phi}{m} T + g + \frac{\theta}{m} T_D \\ \ddot{\theta} &= c_4\dot{\psi}\dot{\phi} - 2\tau_1 K + 2c_7\tau_2 \end{aligned} \tag{22}$$

where $K = c_5 c_\alpha - c_6 s_\alpha$, $T = \tau_1 c_\alpha + \tau_2 + T_L$.

To stabilize the transition mode system (22), the backstepping approach is used to design the control laws $\tau_1$ and $\tau_2$. The basic idea of the backstepping approach is to decompose a complex nonlinear system into several subsystems that do not exceed the system order. Then, design partial Lyapunov

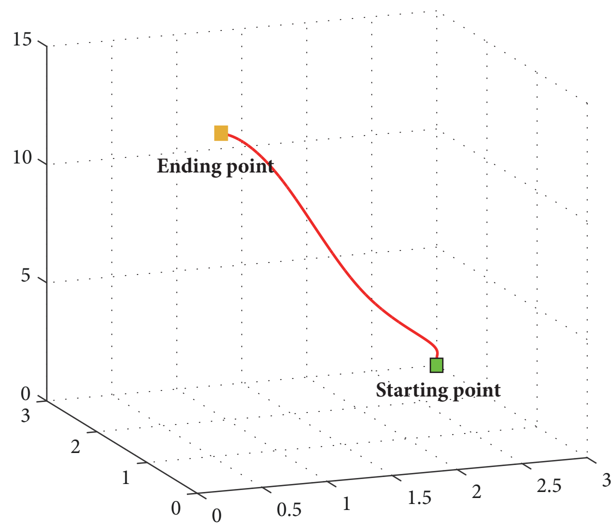


Figure 5: DTR takeoff trajectory.

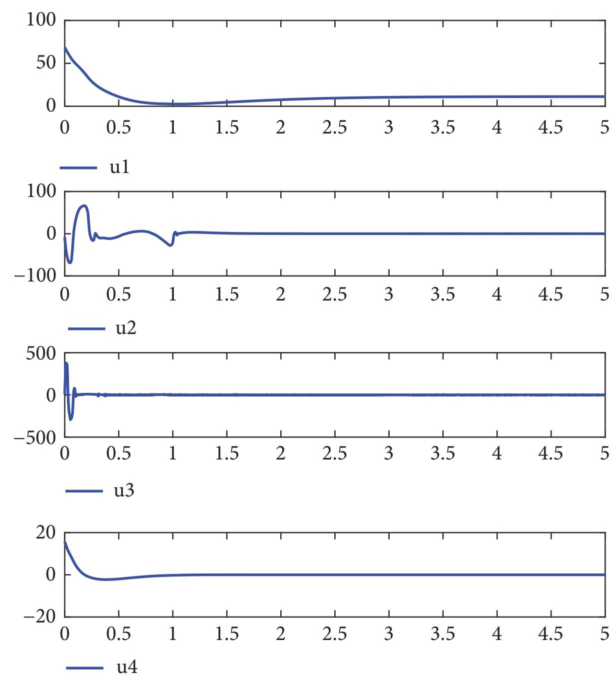


Figure 6: The control inputs of takeoff.

functions and intermediate virtual control for each subsystem until back to the entire system. Finally, they are integrated to complete the design of the entire control law.

**Theorem 1.** *Consider that the transition mode system (22) is a multi-input and multioutput coupling system. The equations of $\ddot{\theta}$ and $\ddot{z}$ could be separated to design the control law, respectively. If $a = m(-z_3 - k_3\dot{z}_3 + g - k_4 z_4) + T_D\theta - 2c_\phi T_L - c_\phi K/c_7$, $b = 2s_\alpha\theta + 2c_\phi c_\alpha + 2c_\phi K/c_7$. The control law can be given as $\tau_1 = a/b$ and $\tau_2 = (k_1\dot{z}_1 + z_1 + k_2 z_2 + 2aK/b)/2c_7$.*

*Proof.* The process of proof will be divided into three parts. In the first part, the Lyapunov function will be constructed and the stability of $\ddot{\theta}$ subsystem will be proved. In the second part, the stability of the $\ddot{z}$ subsystem will be proved. In the third part, the control input of the stabilization system will be given.

*Part I: We Will Prove the Stability of $\ddot{\theta}$ Subsystem.* The pitch subsystem is designed as follows:

$$\begin{aligned} \dot{\omega}_1 &= \omega_2 \\ \dot{\omega}_2 &= c_4\dot{\psi}\dot{\phi} - 2\tau_1 K + 2c_7\tau_2 \end{aligned} \tag{23}$$

where $\omega_1 = \theta$. The virtual input $u_\theta$ is introduced which is equal to the pitch rate $\dot{\omega}_1$. The error of pitch is defined as

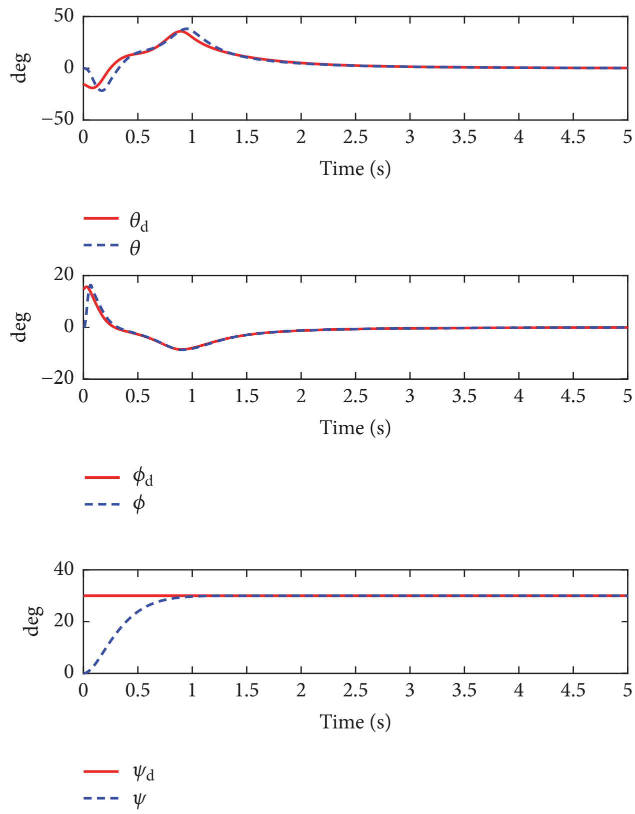


Figure 7: DTR attitude tracking effect.

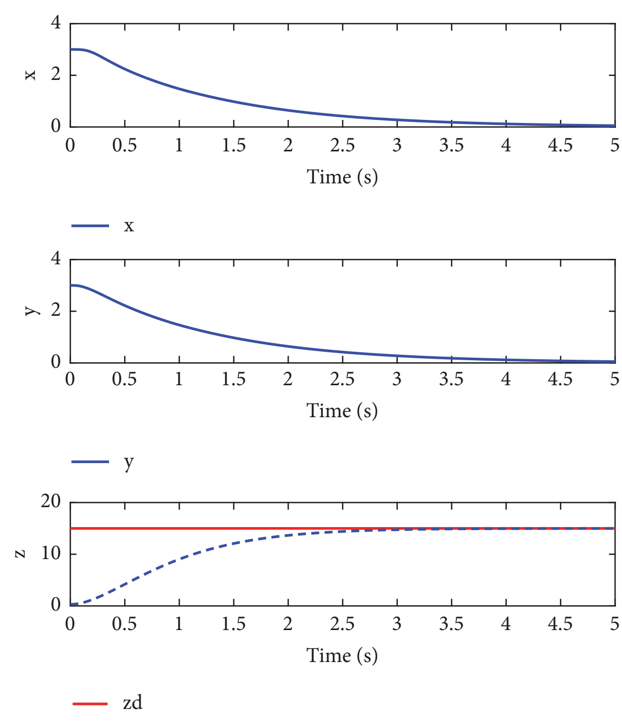


Figure 8: DTR position tracking effect.

$$z_1 = \theta_d - \omega_1 \tag{24}$$

Construct the Lyapunov function,

$$V(z_1) = \frac{1}{2} z_1^2 \tag{25}$$

The derivative of the Lyapunov function is

$$\dot{V}(z_1) = z_1 \dot{z}_1 = -z_1 u_\theta \tag{26}$$

To guarantee $\dot{V}(z_1) < 0$, suppose that

$$u_\theta = k_1 z_1 \tag{27}$$

where $k_1 > 0$. The error of the pitch rate is defined as

$$z_2 = u_\theta - \omega_2 \tag{28}$$

The derivative of $z_2$ is

$$\dot{z}_2 = k_1 \dot{z}_1 - \dot{\omega}_2 \tag{29}$$

And $\dot{z}_1$ can be obtained from (24) and (28),

$$\dot{z}_1 = -k_1 z_1 + z_2 \tag{30}$$

Construct the Lyapunov function,

$$V(z_1, z_2) = \frac{1}{2} z_1^2 + \frac{1}{2} z_2^2 \tag{31}$$

And the derivative of $V(z_1, z_2)$ is

$$\begin{aligned} \dot{V}(z_1, z_2) &= z_1 \dot{z}_1 + z_2 \dot{z}_2 \\ &= z_1 (-k_1 z_1 + z_2) + z_2 (k_1 \dot{z}_1 - \dot{\omega}_2) \end{aligned} \tag{32}$$

To make $\dot{V}(z_1, z_2) < 0$, suppose that

$$k_1 \dot{z}_1 - \dot{\omega}_2 = -k_2 z_2 - z_1 \tag{33}$$

where $k_2 > 0$. Thus,

$$\dot{V}(z_1, z_2) = -k_1 z_1^2 - k_2 z_2^2 \tag{34}$$

And $\dot{V}(z_1, z_2) < 0$ satisfies the condition for system stabilization.

*Part II: We Will Prove the Stability of $\ddot{z}$ Subsystem.* The altitude subsystem is designed as

$$\begin{aligned} \dot{\xi}_1 &= \xi_2 \\ \dot{\xi}_2 &= -2\tau_1 s_\alpha \frac{\theta}{m} - \frac{2c_\phi}{m} T + g + \frac{\theta T_D}{m} \end{aligned} \tag{35}$$

where $\xi_1 = z$. The virtual input $u_z$ is introduced which is equal to the altitude rate $\dot{z}$. The altitude error is defined as

$$z_3 = z_d - \xi_1 \tag{36}$$

Construct the Lyapunov function,

$$V(z_3) = \frac{1}{2} z_3^2 \tag{37}$$

The derivative of the $V(z_3)$ is

$$\dot{V}(z_3) = z_3 \dot{z}_3 = -z_3 u_z \tag{38}$$

Suppose that $u_z = k_3 z_3$. Thus,

$$\dot{V}(z_3) = -k_3 z_3^2 \tag{39}$$

where $k_3 > 0$. The altitude rate error is defined as

$$z_4 = u_z - \xi_2 \tag{40}$$

From (37) and (41) $z_3$ can be obtained as

$$z_3 = -k_3 z_3 + z_4 \tag{41}$$

Construct the Lyapunov function $V(z_3, z_4)$ as

$$V(z_3, z_4) = \frac{1}{2} z_3^2 + \frac{1}{2} z_4^2 \tag{42}$$

The derivative of the $V(z_3, z_4)$ is

$$\begin{aligned} \dot{V}(z_3, z_4) &= z_3 \dot{z}_3 + z_4 \dot{z}_4 \\ &= z_3 (-k_3 z_3 + z_4) + z_4 (k_3 \dot{z}_3 - \dot{\xi}_2) \end{aligned} \tag{43}$$

To make $\dot{V}(z_3, z_4) < 0$, suppose that

$$k_3 \dot{z}_3 - \dot{\xi}_2 = -k_4 z_4 - z_3 \tag{44}$$

where $k_4 > 0$. Thus,

$$\dot{V}(z_3, z_4) = -k_3 z_3^2 - k_4 z_4^2 \tag{45}$$

And $\dot{V}(z_3, z_4) < 0$ satisfies the condition for system stabilization.

*Part III: The Control Inputs Will Be Given.* The first equation of $\tau_1$ and $\tau_2$ can be obtained from (23) and (33),

$$k_1 \dot{z}_1 - c_4 \dot{\psi} \dot{\phi} + 2\tau_1 K - 2c_7 \tau_2 = -k_2 z_2 - z_1 \tag{46}$$

The second equation of $\tau_1$ and $\tau_2$ can be obtained from (35) and (44),

$$k_3 \dot{z}_3 + \frac{2 s_\alpha \theta \tau_1}{m} + \frac{2 c_\phi T}{m} - g - \frac{T_D \theta}{m} = -k_4 z_4 - z_3 \tag{47}$$

Thus, the control law $\tau_1$ and $\tau_2$ can be calculated by (46) and (47),

$$\begin{aligned} \tau_1 &= \frac{a}{b} \\ \tau_2 &= \frac{k_1 \dot{z}_1 + z_1 + k_2 z_2 + 2aK/b}{2c_7} \end{aligned} \tag{48}$$

This proof is completed. □

Table 1: Simulation parameters of the DTR vehicle.

| Parameters | Unit | Value |
|---|---|---|
| m | kg | 4.50 |
| $I_x$ | $kg.m^2$ | 0.039 |
| $I_y$ | $kg.m^2$ | 0.042 |
| $I_z$ | $kg.m^2$ | 0.076 |
| $L_x$ | m | 0.32 |
| $L_y$ | m | 0.30 |
| $L_z$ | m | 0.11 |
| $\rho$ | $kg/m^3$ | 1.29 |
| A | $m_2$ | 0.20 |
| $k_1$ | 1 | 1.20 |
| $k_2$ | 1 | 1.20 |
| $k_3$ | 1 | 2.20 |
| $k_4$ | 1 | 2.20 |

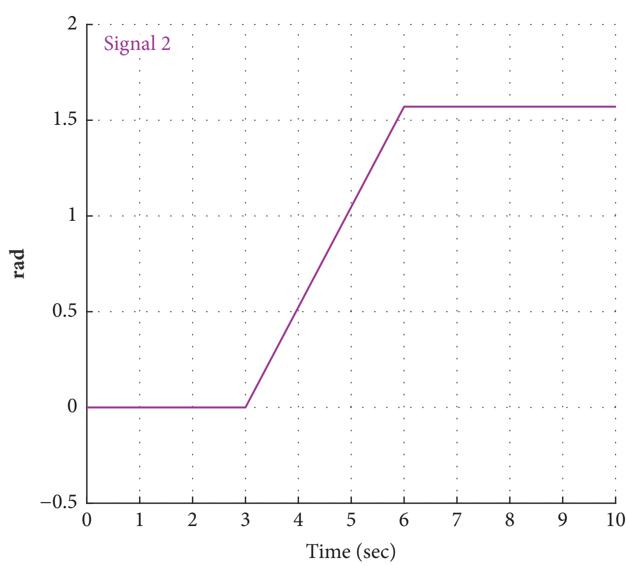


Figure 9: Tilting angle signal source.

The numerical results for the DTR UAV have been showed in Figures 10, 11, and 12. The Figure 9 represents the tilting angle signal source which changes from 0 to $\pi/2$ in 3 to 6 seconds. The system parameters are listed in Table 1.

In Figure 10, the DTR UAV takes off vertically until it reaches the target height $d1 = 15m$. The rotors start to tilt in the 3rd second and end in the 6th second and the height also reaches the reference height $zd2 = 40m$. After transition the vehicle flies horizontally at the reference height. In Figure 11, $\theta$ changes within 10 degrees and eventually converges to 0 from the beginning of the transition to the end. $\phi$ shows a slight changes and $\psi$ slightly deviates from the reference value of the vertical takeoff. However, these tiny changes will not affect the balance of the aircraft. The Figure 12 shows the complete trajectory from takeoff to horizontal flight.

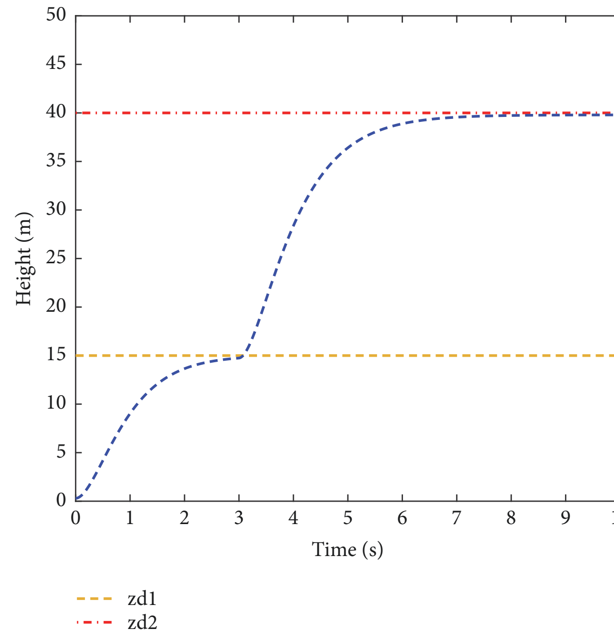


Figure 10: Altitude control during transition mode.

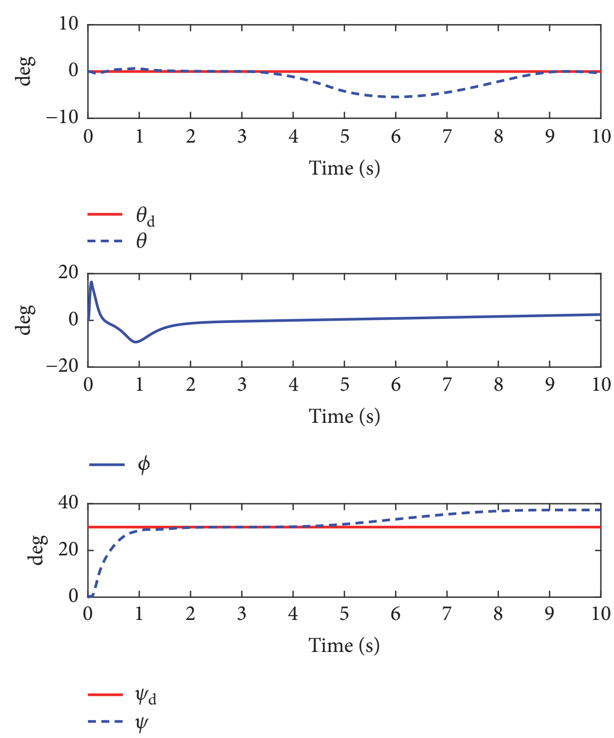


Figure 11: Attitude control during transition mode.

## 5. Experimental Results

The vertical flight experiment was performed on the DTR aircraft platform which is developed at laboratory. The fuselage framework is built by elastomeric polyurethane (EPU) and carbon fiber. The tilting angle is controlled by two actuators. In addition, the DTR aircraft is equipped with GPS, airspeed

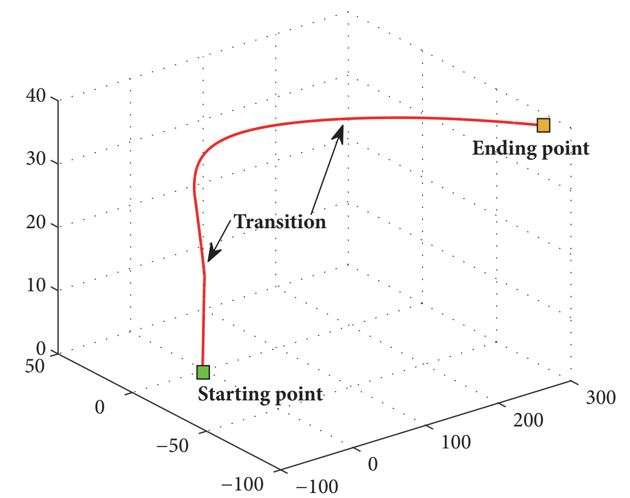


Figure 12: DTR trajectory from takeoff to horizontal flight.

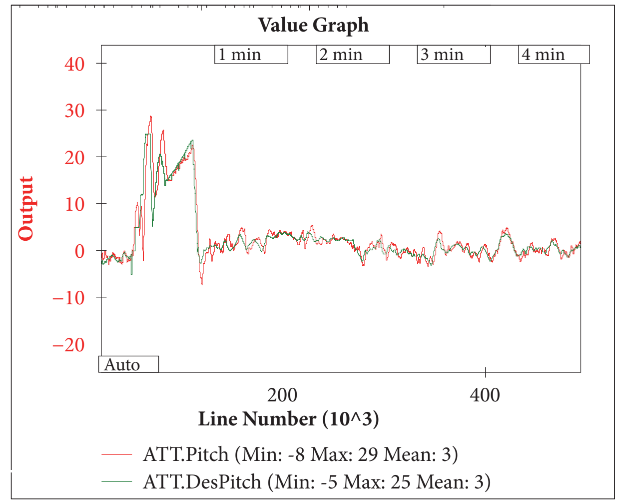


Figure 13: The pitch and desired pitch in experiment.

meter, and antenna for communication with the ground station software. The 10000mha high-rate lithium polymer battery is chosen and connected with electronic governor to supply the rotors. Moreover, the control system integrates 3-axis accelerometer and gyroscope to provide aircraft's attitude. The aircraft is equipped with the high precision digital air pressure sensor MS-5611 used to obtain height and connected with the compass through the I2C interface to calibrate the flight direction. The flight control system is based on PIXHAWK Autopilot. PIXHAWK is a dual-processor flight controller consisting of a 32 bit STM32F427 Cortex M4 core processor which contains 256KB RAM and 2 MB flash and a 32 bit STM32F103 coprocessor which is used to ensure safety when the core processor crashes.

The experiment was conducted in an outdoor environment without wind. The experiment results can be obtained by establishing a connection between the ground station software Mission Planner and the aircraft. The experiment results are showed in Figures 13–16 and Figure 18. Figures 13–16 show the DTR aircraft attitude and flight height. And the DTR aircraft is showed in Figure 17. Figure 18 shows the DTR aircraft's flight in the real experiment and the aircraft flight attitude was stable.

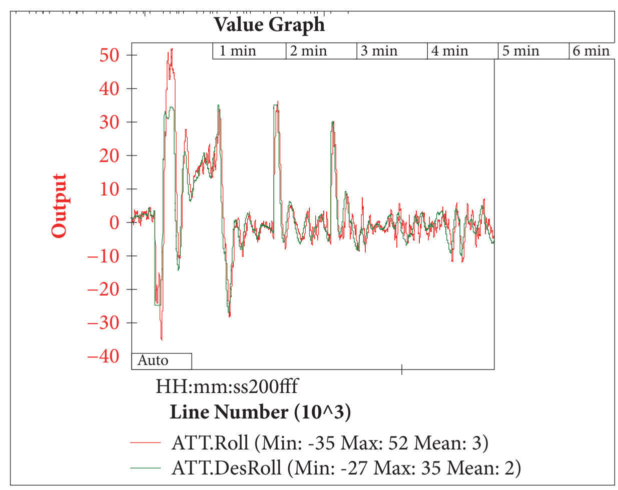


Figure 14: The roll and desired roll in experiment.

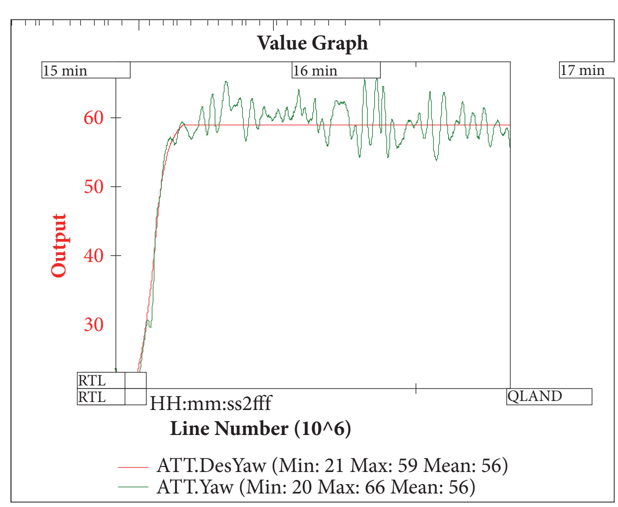


Figure 15: The yaw and desired yaw in experiment.

## 6. Conclusion

A novel tiltrotor aircraft has been presented with two tiltable rotors and two fixed rotors. The kinetics model of the DTR aircraft has been established. And control laws for vertical flight and transition are designed, respectively. The PID controller was designed for the vertical flight and a nonlinear controller based on backstepping approach was designed for the transition. The numerical results have shown the effectiveness of the control approaches for vertical flight and transition. Moreover, the vertical flight experiment was performed on the DTR aircraft platform and the flight attitude was stable. In this part of work, wind disturbance is not considered. Therefore, the robustness of the proposed

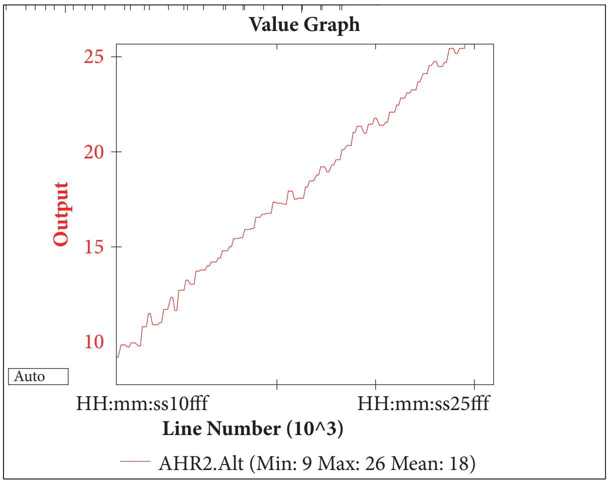


Figure 16: The flight height of the DTR aircraft.


Figure 17: Overview of the developed DTR aircraft.

Figure 18: The DTR aircraft vertical flight experiment.

approach needs to be further verified. The elevator and rudder are not used during the transition and the DTR aircraft attitude is completely controlled by rotors. In the next work, the disturbance will be considered into the kinetics model. The elevator and rudder will also be used to control the attitude of the DTR aircraft.

## Data Availability

The data used to support the findings of this study are available from the corresponding author upon request.

## Conflicts of Interest

The authors declare that they have no conflicts of interest.

## Acknowledgments

This work was supported in part by the Zhejiang Provincial Natural Science Foundation of China under Grant LY18F030008 and the National Natural Science Foundation of China under Grant 61375104.

## References

[1] C.-C. Yih, "Flight control of a tilt-rotor quadcopter via sliding mode," in *Proceedings of the 2016 International Automatic Control Conference, CACS 2016*, pp. 65–70, Taichung, Taiwan, November 2016.

[2] K. T. Oner, E. Cetinsoy, E. Sirimoglu, C. Hancer, T. Ayken, and M. Unel, "LQR and SMC stabilization of a new unmanned aerial vehicle," *World Academy of Science, Engineering and Technology*, vol. 58, pp. 373–378, 2009.

[3] K. Benkhoud and S. Bouallègue, "Model predictive control design for a convertible Quad Tilt-Wing UAV," in *Proceedings of the 2016 4th International Conference on Control Engineering & Information Technology (CEIT)*, pp. 1–6, Hammamet, Tunisia, December 2016.

[4] G. Flores and R. Lozano, "Transition flight control of the quad-tilting rotor convertible MAV," in *Proceedings of the 2013 International Conference on Unmanned Aircraft Systems, ICUAS 2013*, pp. 789–794, Atlanta, Ga, USA, May 2013.

[5] G. R. Flores-Colunga and R. Lozano-Leal, "A nonlinear control law for hover to level flight for the Quad Tilt-rotor UAV," *IFAC Proceedings Volumes*, vol. 47, no. 3, pp. 11055–11059, 2014.

[6] F. Kendoul, I. Fantoni, and R. Lozano, "Modeling and control of a small autonomous aircraft having two tilting rotors," in *Proceedings of the 44th IEEE Conference on Decision and Control, and the European Control Conference, CDC-ECC '05*, pp. 8144–8149, Seville, Spain, December 2005.

[7] K. Benkhoud, S. Bouallègue, and M. Ayadi, "Rapid control prototyping of a quad-tilt-wing unmanned aerial vehicle," in *Proceedings of the 2017 International Conference on Control, Automation and Diagnosis, ICCAD 2017*, pp. 423–428, Hammamet, Tunisia, January 2017.

[8] C. Hancer, K. T. Oner, E. Sirimoglu, E. Cetinsoy, and M. Unel, "Robust hovering control of a quad tilt-wing UAV," in *Proceedings of the 36th Annual Conference of the IEEE Industrial Electronics Society, IECON 2010*, pp. 1615–1620, Glendale, Ariz, USA, November 2010.

[9] M. Sato and K. Muraoka, "Control performance improvement for QTW UAV by using feedforward gains," in *Proceedings of the 54th Annual Conference of the Society of Instrument and Control Engineers of Japan, SICE 2015*, pp. 824–829, Hangzhou, China, July 2015.

[10] S. Suzuki, R. Zhijia, Y. Horita et al., "Attitude control of quad rotors QTW-UAV with tilt wing mechanism," *Journal of System Design & Dynamics*, vol. 4, no. 3, pp. 416–428, 2007.

[11] T. Mikami and K. Uchiyama, "Design of flight control system for quad tilt-wing UAV," in *Proceedings of the 2015 International Conference on Unmanned Aircraft Systems, ICUAS 2015*, pp. 801–805, Denver, Colo, USA, June 2015.

[12] Q. Lin, Z. Cai, J. Yang, Y. Sang, and Y. Wang, "Trajectory tracking control for hovering and acceleration maneuver of Quad Tilt Rotor UAV," in *Proceedings of the 33rd Chinese Control Conference, CCC 2014*, pp. 2052–2057, Nanjing, China, July 2014.

[13] J. Lee, C. Yoo, Y.-S. Park et al., "An experimental study on time delay control of actuation system of tilt rotor unmanned aerial vehicle," *Mechatronics*, vol. 22, no. 2, pp. 184–194, 2012.

[14] X. Wang and L. Cai, "Mathematical modeling and control of a tilt-rotor aircraft," *Aerospace Science and Technology*, vol. 47, no. 12, pp. 473–492, 2015.

[15] S. Park, J. Bae, Y. Kim, and S. Kim, "Fault tolerant flight control system for the tilt-rotor UAV," *Journal of The Franklin Institute*, vol. 350, no. 9, pp. 2535–2559, 2013.

[16] G. Flores, I. Lugo, and R. Lozano, "6-DOF hovering controller design of the Quad Tiltrotor aircraft: Simulations and experiments," in *Proceedings of the 2014 53rd IEEE Annual Conference on Decision and Control, CDC 2014*, pp. 6123–6128, Los Angeles, Calif, USA, December 2014.

[17] A. Nemati and M. Kumar, "Modeling and control of a single axis tilting quadcopter," in *Proceedings of the 2014 American Control Conference, ACC 2014*, pp. 3077–3082, Portland, Ore, USA, June 2014.

[18] E. Altug, J. Ostrowski, and R. Mahony, "Control of a quadrotor helicopter using visual feedback," in *Proceedings of the International Conference on Robotics & Automation*, vol. 1, pp. 72–77, Washington, Wash, USA, 2002.

[19] H. Liu, Y. Bai, G. Lu, Z. Shi, and Y. Zhong, "Robust tracking control of a quadrotor helicopter," *Journal of Intelligent & Robotic Systems*, vol. 75, no. 3-4, pp. 595–608, 2014.

[20] T. Hamel, R. Mahony, and A. Chriette, "Visual servo trajectory tracking for a four rotor VTOL aerial vehicle," in *Proceedings of the EEE International Conference on Robotics & Automation*, vol. 3, pp. 2781–2786, Washington, Wash, USA.

[21] E. Kayacan and R. Maslim, "Type-2 fuzzy logic trajectory tracking control of quadrotor VTOL aircraft with elliptic membership functions," *IEEE/ASME Transactions on Mechatronics*, vol. 22, no. 1, pp. 339–348, 2017.

[22] R. Xu and Ü. Özgüner, "Sliding mode control of a class of underactuated systems," *Automatica*, vol. 44, no. 1, pp. 233–241, 2008.

[23] C. Papachristos, K. Alexis, and A. Tzes, "Hybrid model predictive flight mode conversion control of unmanned Quad-TiltRotors," in *Proceedings of the 2013 12th European Control Conference, ECC 2013*, pp. 1793–1798, Zurich, Switzerland, July 2013.